SU(3) analysis for *B*(*E*2) anomaly

Yu-xin Cheng (程宇欣)[1] De-hao Zhao (赵德浩)[1] Yue-yang Shao (邵跃洋)[2] Li Gong (龚丽)[1]
Tao Wang (王涛)[2†] Xiao-shen Kang (康晓珅)[1‡]

[1]School of Physics, Liaoning University, Shenyang 110036, China
[2]College of Physics, Tonghua Normal University, Tonghua 134000, China

Abstract: The concept of "*SU*(3) analysis" is proposed for the *B*(*E*2) anomaly based on various mechanisms reported recently. The *B*(*E*2) anomaly is analyzed in the *SU*(3) symmetry limit. According to the results of the analysis, the *SU*(3) third-order interaction $[L\times Q\times L]^{(0)}$ can generate the level-crossing phenomenon for any mechanism, which is vital for the emergence of the *B*(*E*2) anomaly. Thus, this anomaly is found to be related with the *SU*(3) symmetry. The *B*(*E*2) anomaly in ^{168}Os is also analyzed.

Keywords: *B*(*E*2) anomaly, SU3-IBM, *SU*(3) analysis, level-crossing

DOI: 10.1088/1674-1137/aded05 **CSTR:** 32044.14.ChinesePhysicsC.49104105

I. INTRODUCTION

Understanding the deformations of nuclei and how they change, whether continuously or abruptly, is one of the fundamental problems in nuclear structure. Quadrupole deformations are the most significant. A geometrical model with deformation variables β and γ provides a good description, where β represents the degree of deviation from the spherical shape and γ represents the angle that describes the triaxial deformation. Fifty years ago, the interacting boson model (IBM) was proposed [1, 2], which is an algebraic model for describing the collective excitations (deformations) in the nuclear structure. For the simplest case, only the *s* and *d* bosons with angular momentum $L=0$ and $L=2$, respectively, are considered to construct the Hamiltonian, which features the *U*(6) symmetry. Four dynamical symmetry limits exist: *U*(5) symmetry (spherical shape), *SU*(3) symmetry (prolate shape), *O*(6) symmetry (γ-soft rotation), and $\overline{SU(3)}$ symmetry (oblate shape) [3]. Shape phase transitions between different shapes can also be studied using this model [4−18]. Thus, the IBM provides an efficient theoretical framework to describe various deformations of nuclei and their collective excitation behaviors, and it has a broad impact in the field of nuclear structure.

Although the IBM is self-consistent for describing various quadrupole deformations, some experimental anomalies appear to be indescribable by previous model Hamiltonians, such as the *B*(*E*2) anomaly [19−22] and Cd puzzle [23−28]. In the *B*(*E*2) anomaly, the ratio $E_{4/2}=E_{4_1^+}/E_{2_1^+}$ of the energies for the 4_1^+, 2_1^+ states is greater than 2.0 (a feature for the collective excitations). However, the ratio $B_{4/2}=B(E2;4_1^+\to 2_1^+)/B(E2;2_1^+\to 0_1^+)$ of the *E*2 transitions $B(E2;4_1^+\to 2_1^+)$ and $B(E2;2_1^+\to 0_1^+)$ can be much smaller than 1.0 (a traditional signal for non-collective behaviors), which cannot be possibly explained by previous theories on nuclear structure [19−22]. Regarding the Cd puzzle, the experimental data did not confirm the phonon excitations of the spherical nucleus [23−27], thereby questioning their existence [28]. Experimentally, the *B*(*E*2) anomaly and Cd puzzle can occur in adjacent nuclei, such as $^{72-76}$Zn [29−31], and even in a single nucleus, such as ^{114}Te [32, 33]. Therefore, they may have a common origin.

Moreover, it was found that nuclei previously considered to have a prolate shape should be rigid triaxial [34−36], making previous IBM descriptions not particularly convenient. In such descriptions, the spectra of the prolate (*SU*(3) symmetry limit) and oblate ($\overline{SU(3)}$ symmetry limit) shapes are the same [3]. However, this mirror symmetry cannot be found in realistic nuclei [37].

Therefore, it is necessary to further generalize upon the existing models. Recently, an extension of the interacting boson model with *SU*(3) higher-order interactions (SU3-IBM) was proposed to resolve the aforementioned various anomalies. In the SU3-IBM, by introducing the *SU*(3) third-order and fourth-order interactions, the *SU*(3) symmetry limit can describe both prolate (*SU*(3) second Casimir operator $-\hat{C}_2[SU(3)]$) and oblate ($\hat{C}_3[SU(3)]$) shapes as well as various rigid triaxial shapes (combinations of $-\hat{C}_2[SU(3)]$, $\hat{C}_3[SU(3)]$, and $\hat{C}_2^2[SU(3)]$), and even

Received 16 April 2025; Accepted 7 July 2025; Published online 8 July 2025
† E-mail: suiyueqiaoqiao@163.com
‡ E-mail: kangxiaoshen@lnu.edu.cn

dynamical effects independent of the ground state. Thus, the $SU(3)$ symmetry plays a more important role.

Through detailed analysis, it was found that this model can better describe the collective behaviors of atomic nuclei. In particular, it can describe the $B(E2)$ anomaly and Cd puzzle [38, 39]. Although the $B(E2)$ anomaly cannot be described by previous nuclear theories [19−22], many possible explanations have been proposed in the SU3-IBM and other extended IBM theories [40−48]. The spherical-like spectra for resolving the Cd puzzle were actually found in ^{106}Pd [49]. The SU3-IBM can also be used to explain the prolate-oblate shape asymmetric transitions in the Hf-Hg region [50−52], to better describe the γ-soft behaviors in ^{196}Pt [53], to describe the E(5)-like spectra in ^{82}Kr [54], and to explain the unique boson number odd-even phenomenon in $^{196-204}$Hg [55], which was first reported in Ref. [51]. Furthermore, it can well describe the rigid triaxiality in ^{166}Er [56]. Recently, the shape phase transition from the new γ-soft phase to the prolate shape was also reported, with ^{108}Pd being the critical nucleus [57]. These results have overturned our traditional understanding of nuclear structure, as they have captured nearly all shape patterns and provided new collective patterns for describing various anomalous behaviors.

Based on previous studies [40−48], discussions on the mechanisms underlying the $B(E2)$ anomaly continue. To date, many possible explanations have been proposed for this anomaly. More fundamental discussions could clarify certain key parts. We introduce the concept "$SU(3)$ analysis," which is applied to re-analyze the results obtained in these studies within the $SU(3)$ symmetry limit. We remove the non-$SU(3)$ symmetry parts of the Hamiltonian to discuss whether the remaining $SU(3)$ symmetry part can have the $B(E2)$ anomaly ($B(E2;4_1^+ \to 2_1^+) = 0$). If this is the case, it may be the reason for the emergence of the $B(E2)$ anomaly in the original Hamiltonian. For the remaining $SU(3)$ symmetry part, we assume that the parameter in front of the $SU(3)$ third-order interaction $[L\times Q\times L]^{(0)}$ varies, and the partial low-lying levels and values of $B(E2;2_1^+ \to 0_1^+)$, $B(E2;4_1^+ \to 2_1^+)$ and $B(E2;6_1^+ \to 4_1^+)$ are analyzed. We found three new results: (1) The interaction $[L\times Q\times L]^{(0)}$ is critical for the $SU(3)$ anomaly, (2) level-crossing within the $SU(3)$ symmetry limit is crucial for the $SU(3)$ anomaly, and (3) not only the value of $B(E2;4_1^+ \to 2_1^+)$ but also those of $B(E2;6_1^+ \to 4_1^+)$ and $B(E2;2_1^+ \to 0_1^+)$can be anomalous (these values can be 0). Thus, $SU(3)$ analysis is a useful tool for identifying the real cause. We expect it can be used in future discussions on the $B(E2)$ anomaly.

II. SU3-IBM HAMILTONIAN

In the SU3-IBM, the $U(5)$ symmetry and $SU(3)$ symmetry limits are included (some bias towards the $O(6)$ symmetry may be also required). In the $SU(3)$ symmetry limit, the $SU(3)$ second-order Casimir operator $-\hat{C}_2[SU(3)]$ can describe the prolate shape and the $SU(3)$ third-order Casimir operator $\hat{C}_3[SU(3)]$ can describe the oblate shape, which is the fundamental difference from the previous IBM [52]. The rigid triaxial shape can be obtained by the combinations of the square of the $SU(3)$ second-order Casimir operator $\hat{C}_2^2[SU(3)]$ and $-\hat{C}_2[SU(3)]$, $\hat{C}_3[SU(3)]$. Moreover, the $SU(3)$ invariants $[L\times Q\times L]^{(0)}$ and $[(L\times Q)^{(1)}\times(L\times Q)^{(1)}]^{(0)}$ are necessary.

The Hamiltonian is as follows:

$$\begin{aligned}\hat{H} = {} & \alpha\hat{n}_d + \beta\hat{C}_2[SU(3)] + \gamma\hat{C}_3[SU(3)] + \delta\hat{C}_2^2[SU(3)] \\ & + \eta[\hat{L}\times\hat{Q}\times\hat{L}]^{(0)} + \zeta[(\hat{L}\times\hat{Q})^{(1)}\times(\hat{L}\times\hat{Q})^{(1)}]^{(0)} \\ & + \xi\hat{L}^2, \end{aligned} \tag{1}$$

where α, β, γ, δ, η, ζ, and ξ are fitting parameters; $\hat{n}_d = d^\dagger\cdot\tilde{d}$ is the d boson number operator; $\hat{Q} = [d^\dagger\times\tilde{s} + s^\dagger\times\tilde{d}]^{(2)} - \frac{\sqrt{7}}{2}[d^\dagger\times\tilde{d}]^{(2)}$ is the $SU(3)$ quadrupole operator; and $\hat{L} = \sqrt{10}[d^\dagger\times\tilde{d}]^{(1)}$ is the angular momentum operator. The first four interactions determine the quadrupole shapes of the ground state of the nucleus and the positions of the 0^+ states of the excited levels. The remaining three ones are dynamical interactions and can be used to change the features of the non-0^+ states.

The two $SU(3)$ Casimir operators are related with the quadrupole second- or third-order interactions as follows:

$$\hat{C}_2[SU(3)] = 2\hat{Q}\cdot\hat{Q} + \frac{3}{4}\hat{L}\cdot\hat{L}, \tag{2}$$

$$\hat{C}_3[SU(3)] = -\frac{4}{9}\sqrt{35}[\hat{Q}\times\hat{Q}\times\hat{Q}]^{(0)} - \frac{\sqrt{15}}{2}[\hat{L}\times\hat{Q}\times\hat{L}]^{(0)} \tag{3}$$

For a given $SU(3)$ irreducible representation (λ,μ), the eigenvalues of the two Casimir operators under the group chain $U(6)\supset SU(3)\supset O(3)$ are expressed as

$$\hat{C}_2[SU(3)] = \lambda^2 + \mu^2 + \mu\lambda + 3\lambda + 3\mu, \tag{4}$$

$$\hat{C}_3[SU(3)] = \frac{1}{9}(\lambda-\mu)(2\lambda+\mu+3)(\lambda+2\mu+3). \tag{5}$$

The $SU(3)$ irreducible representation (λ,μ) can be related with the quadrupole deformation variables β and γ as

$$\beta = \beta_0\sqrt{\lambda^2+\mu^2+\lambda\mu+3\lambda+3\mu}, \tag{6}$$

and

$$\gamma = \tan^{-1}\left(\frac{\sqrt{3}(\mu+1)}{2\lambda+\mu+3}\right), \tag{7}$$

where β_0 is a scale factor.

For understanding the *B*(*E*2) anomaly, the *B*(*E*2) values are necessary. The *E*2 operator is defined as

$$\hat{T}(E2) = q\hat{Q}, \tag{8}$$

where q is the boson effective charge. The evolutions of $B(E2;2_1^+ \to 0_1^+)$, $B(E2;4_1^+ \to 2_1^+)$, and $B(E2;6_1^+ \to 4_1^+)$ values are discussed.

III. *SU*(3) ANALYSIS

The *B*(*E*2) anomaly cannot be explained by previous nuclear structure theories. However, in the extended IBM with higher-order interactions, it can be described using different approaches [40−48]. A key problem is to determine whether these explanations are related with the *SU*(3) symmetry. Evidently, these explanations must be considered in the *SU*(3) symmetry limit. To explain the *B*(*E*2) anomaly in realistic nuclei, the boson number operator $\hat{n}_d$ is needed in some descriptions or the *SU*(3) quadrupole operator $\hat{Q}$ is replaced by the generalized quadrupole operator $\hat{Q}_\chi = [d^\dagger \times \tilde{s} + s^\dagger \times \tilde{d}]^{(2)} + \chi[d^\dagger \times \tilde{d}]^{(2)}$ (some bias towards the *O*(6) symmetry means $\chi \neq -\frac{\sqrt{7}}{2}$). Thus, for *SU*(3) analysis, the $\hat{n}_d$ interaction should be removed (here $\alpha_- = 0$), and $\hat{Q}_\chi$ is replaced by $\hat{Q}$ again (here $\chi = -\frac{\sqrt{7}}{2}$). The non-*SU*(3) symmetry parts are removed. If these operations are feasible, the *SU*(3) analysis exists, which is important for understanding the emergence of the *B*(*E*2) anomaly. This analysis has been ignored in previous studies. In this study, we demonstrate that it is critical.

The *B*(*E*2) anomaly implies that $B_{4/2} < 1.0$ while $E_{4/2} \geq 2.0$. These two quantities involve only 0_1^+, 2_1^+, and 4_1^+ states; therefore, they are important for the success of any nuclear structure theories. This point is similar to the magic number in atomic nuclei, which is only related with the 0_1^+ and 2_1^+ states. It should be noticed that this *B*(*E*2) anomaly was first theoretically reported in Ref. [58], but it is not consistent with the experimental data reported in Refs. [19−22], in which the $B_{4/2}$ values are much smaller than 1.0, even reaching 0.33. We found that the *B*(*E*2) anomaly is a phenomenon as important as that of magic numbers. If a theory cannot explain the *B*(*E*2) anomaly, it is insufficient.

Through numerous careful calculations, we found that the *SU*(3) cubic interaction $[L \times Q \times L]^{(0)}$ plays an important role in explaining the *B*(*E*2) anomaly. (Whether this relationship is unique is still unclear). Thus, when discussing the problem, we let the coefficient η of this interaction change and analyze the characteristics of the *B*(*E*2) anomaly.

IV. ANALYSIS RESULTS

A. First example

Next, we discuss the first example using *SU*(3) analysis. Fig. 1(a) shows the evolutional behaviors of the partial low-lying levels as a function of η in the *SU*(3) symmetry limit in Ref. [40]. This is the first successful explanation for the *B*(*E*2) anomaly of realistic nucleus ^{170}Os. The boson number is $N = 9$. In Ref. [40], the parameters are $\alpha = 302.4$ keV, $\beta = -30.09$ keV, $\gamma = 3.79$ keV, $\delta = 0.0$ keV, $\eta = -10.38$ keV, $\zeta = 0.0$ keV, and $\xi = 18.66$ keV. For *SU*(3) analysis, let $\alpha = 0$. The ground state is a prolate shape with *SU*(3) irrep (18,0). In that previous study, the two *SU*(3) third-order interactions were con-

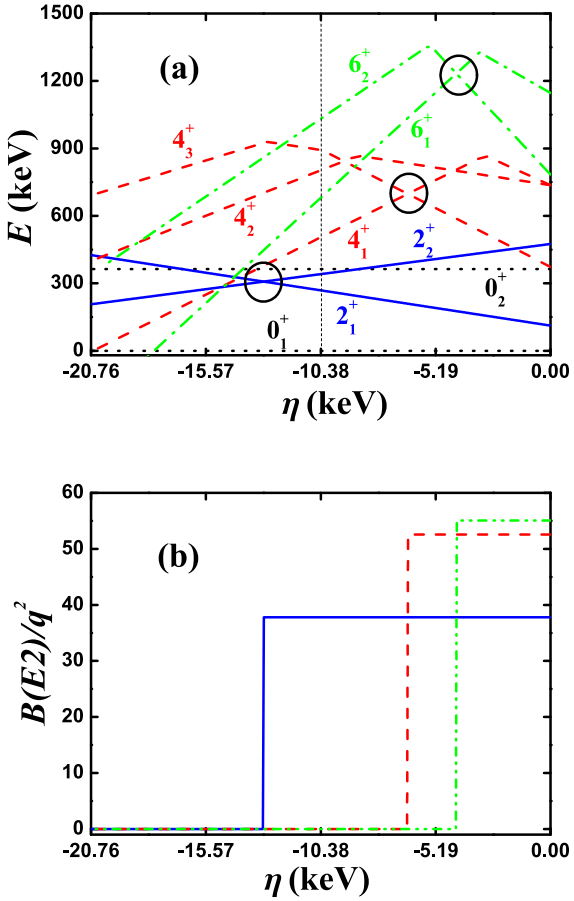

Fig. 1. (color online) (a) Evolutional behaviors of the partial low-lying levels as functions of η; (b) evolutional behaviors of $B(E2;2_1^+ \to 0_1^+)$ (blue real line), $B(E2;4_1^+ \to 2_1^+)$ (red dashed line), and $B(E2;6_1^+ \to 4_1^+)$(green dashed dotted line) as functions of η. The parameters were deduced from Ref. [40].

sidered, unlike the two four-order interactions. From Fig. 1(a), we can see that when η varies from 0 to −20.76 keV (the middle point $\eta = -10.38$ keV is the parameter used in Ref. [40]), the red dashed line of the 4_1^+ state intersects with that of another 4^+ state at $\eta = -6.45$ keV (the crossover point is marked by the black circle, and the latter ones are also the same). In Ref. [40], it was reported that the 4^+ state in the $SU(3)$ irrep (10,4) becomes lower than the 4^+ state in the $SU(3)$ irrep (18,0). In Fig. 1(a), we observe new features that were not observed in previous studies. The 6_1^+ state intersects with the other 6^+ state at $\eta = -4.25$ keV (green dashed dotted lines) and importantly, the 2_1^+ state intersects with the other 2^+ state at $\eta = -12.97$ keV (blue real lines), all marked by black circles. Therefore, we are reporting new results.

A key question, which has been noted but not emphasized in previous studies, is that the new energy spectra still appear to be ordered and are similar to the conventional ones. It seems natural to put the nuclei ^{172}Pt, ^{168,170}Os , and ^{166}W with the $B(E2)$ anomaly into the entire isotopic evolutions (see Refs. [19−22]). However, the $B(E2)$ values suddenly change. This is a subtle point that we would like to emphasize. The thin dashed line at the middle ($\eta = -10.38$ keV) in Fig. 1(a) represents the energy spectra in the $SU(3)$ symmetry limit discussed in Ref. [40]. It can be seen that although level-crossing occurs, the change in the positions of the energy levels is negligible (compared with those at $\eta = 0$). Unless the selected parameter is too large, the energy levels are still in order. If the $\hat{n}_d$ interaction is added, the changes can be less significant. This approximate mirror effect is interesting and will be addressed in the future.

In the $SU(3)$ symmetry limit, if two states belong to different $SU(3)$ irreps., the E2 transitions between them must be 0. Fig. 1(b) shows the evolutional behaviors of $B(E2;2_1^+ \to 0_1^+)$, $B(E2;4_1^+ \to 2_1^+)$, and $B(E2;6_1^+ \to 4_1^+)$ as functions of η. Note that the $B(E2;4_1^+ \to 2_1^+)$ anomaly (here anomaly means that the $E2$ transition is 0) can appear when $\eta \le -6.45$ keV. Note also that the $B(E2;6_1^+ \to 4_1^+)$ anomaly can appear when $\eta \le -4.25$ keV and the $B(E2;2_1^+ \to 0_1^+)$ anomaly can appear when $\eta \le -12.97$ keV. These anomalies are not mentioned in previous studies. Importantly, we found that they really exist in realistic nuclei, such as the $B(E2;6_1^+ \to 4_1^+)$ anomaly for ^{72}Zn [29] and $B(E2;2_1^+ \to 0_1^+)$ anomaly for ^{166}Os [59]. We conclude that the $B(E2;2_1^+ \to 0_1^+)$ anomaly in ^{166}Os is critical for understanding the reason why the $B(E2)$ anomaly occurs in realistic nuclei. The $B(E2;2_1^+ \to 0_1^+)$ anomaly in ^{166}Os has been discussed within a general explanatory framework [60].

Clearly, $SU(3)$ analysis is a powerful technique to understand the $B(E2)$ anomaly. Within the $SU(3)$ symmetry limit, the level-crossing phenomena can occur owing to the $[L \times Q \times L]^{(0)}$ interaction. If the two levels belong to different $SU(3)$ irreps., the $E2$ transition must be 0. This case is different from the $SU(3)$ corresponding to the rigid triaxial description reported in Ref. [58].

B. Second example

Ref. [41] continued to use the rigid triaxial description. Here, we use ^{168}Os for $SU(3)$ analysis. The $SU(3)$ corresponding to the rigid triaxial description was reported in Refs. [61−63]. Then, it was used in the IBM to remove the degeneracy of the β and γ bands [64] and to describe the rigid triaxial spectra [65]. A key step is that Ref. [50] analyzed the extended cubic Q-consistent Hamiltonian and found a new evolutional path from prolate to oblate shapes. This asymmetric shape evolution was also analytically studied in Ref. [51]. In Ref. [58], the $B(E2)$ anomaly was first found theoretically by studying the rigid triaxial rotor. Unfortunately, the authors did not realize that realistic nuclei can exhibit such features in practice. The main result in Ref. [58] is that, when the angular moment L in the ground band increases, the $E2$ transitional values $B(E2;L_1^+ \to (L-2)_1^+)$ really decrease, but they initially decrease slowly, fufilling $B_{4/2} > 0.5$.

For ^{168}Os, the boson number is $N = 8$. The parameters in Fig. 2 , deduced from Ref. [41], are $\alpha = 22$ keV, $\beta = 96$ keV, $\gamma = 27$ keV, $\delta = 0.3$ keV, $\eta = 53$ keV, $\zeta = -45$ keV, and $\xi = 94$ keV. For $SU(3)$ analysis, let $\alpha = 0$. Fig. 2(a) shows the evolutional behaviors of the partial low-lying levels as functions of η from 0 to 106 keV; the middle point is the parameter reported in Ref. [41] ($\eta = 53$ keV). Note that the 4_1^+ state does not intersect with other 4^+ states (red dashed lines), but the 6_1^+ state intersects with one other 6^+ state (green dashed dotted lines and black circle). As shown in Fig. 2(b), the $B(E2;4_1^+ \to 2_1^+)$ value can be lower than the $B(E2;2_1^+ \to 0_1^+)$ value. Thus, the $B(E2)$ anomaly exists and results from the rigid triaxial rotor effect. However, the ratio $B_{4/2}$ is 0.6 at the middle point, larger than the experimental value 0.34. The fact that the rigid triaxial rotor effect can give rise to such a small $B_{4/2}$ value is a problem that should be studied in the future. Clearly, the $B(E2;6_1^+ \to 4_1^+)$ anomaly results from the level-crossing effect. Here, the $SU(3)$ irrep of the ground state is (4,6) ($\gamma = 35.6°$ according to Eq. (7)). Therefore, the $B(E2)$ values are smaller than those in Fig. 1(b) if they exist. Recently, Refs. [47, 48] reported that the small $B(E2)$ anomaly can be found for the rigid triaxial rotor in the IBM-2, which distinguishes between protons and neutrons. In the SU3-IBM, protons and neutrons can also be distinguished, and more complex mechanisms can be found for the $B(E2)$ anomaly.

C. Third example

In Ref. [41], another group of parameters for ^{168}Os was reported: $\alpha = 99$ keV, $\beta = 50.4$ keV, $\gamma = 3.5$ keV, $\delta = 0.55$ keV, $\eta = 43$ keV, $\zeta = -9.7$ keV, and $\xi = 26$ keV. For $SU(3)$ analysis, let $\alpha = 0$. Fig. 3(a) shows the

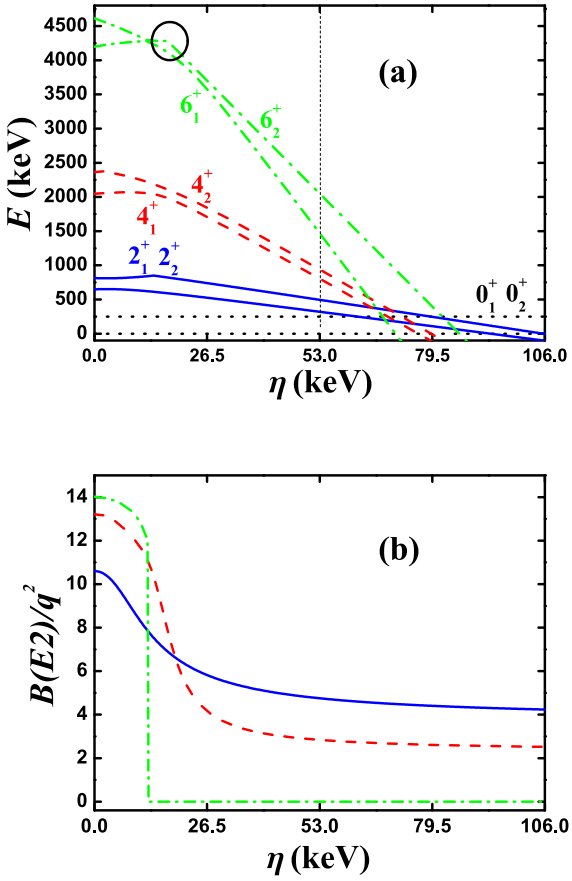

Fig. 2. (color online) (a) Evolutional behaviors of the partial low-lying levels as functions of η; (b) evolutional behaviors of $B(E2;2_1^+\to 0_1^+)$ (blue real line), $B(E2;4_1^+\to 2_1^+)$ (red dashed line), and $B(E2;6_1^+\to 4_1^+)$ (green dashed dotted line) as functions of η. The parameters were deduced from Ref. [41].

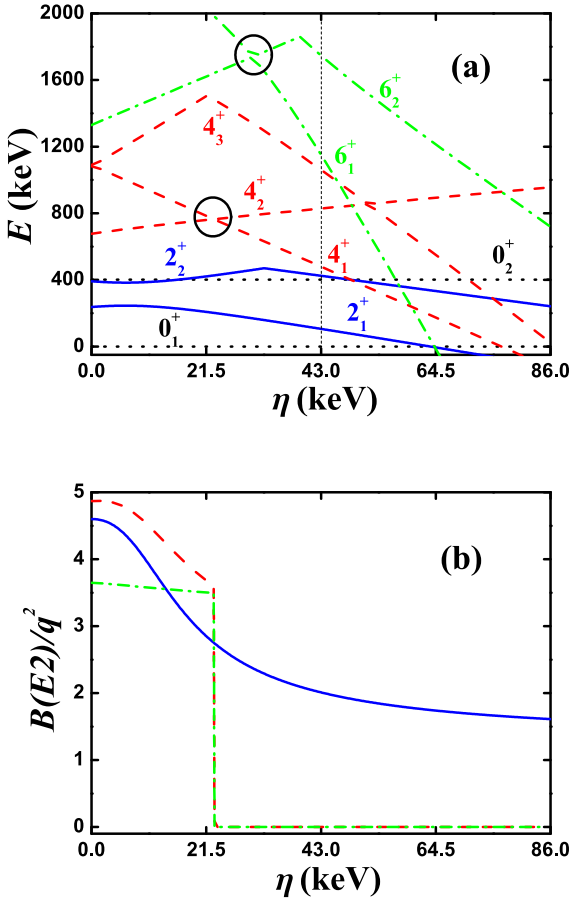

Fig. 3. (color online) (a) Evolutional behaviors of the partial low-lying levels as functions of η; (b) Evolutional behaviors of $B(E2;2_1^+\to 0_1^+)$ (blue real line), $B(E2;4_1^+\to 2_1^+)$ (red dashed line), and $B(E2;6_1^+\to 4_1^+)$ (green dashed dotted line) as functions of η. The parameters were deduced from Ref. [41].

evolutional behaviors of the partial low-lying levels as functions of η from 0 to 86 keV, and the middle point is the parameter reported in Ref. [41] ($\eta = 43$ keV). Clearly, the 4_1^+ state intersects with one other 4^+ state at $\eta = 23$ keV (red dashed lines) and the 6_1^+ state intersects with one other 6^+ state at $\eta = 30.1$ keV (green dashed dotted lines), which is larger than that of the 4^+ states at the crossing point (two black circles). Thus, this $B(E2)$ anomaly results from level-crossing effects. However, these crossing effects may be complex. Thus, confirming real crossing effects in experimental results requires more experimental data. If this is the case, the emergence of the $B(E2)$ anomaly may be an accidental effect. In Fig. 3(b), the $B(E2;4_1^+\to 2_1^+)$ and $B(E2;6_1^+\to 4_1^+)$ anomalies occur simultaneously. The $SU(3)$ irrep. of the ground state is (2,4) ($\gamma = 35.8°$ according to Eq. (7)); therefore, the $B(E2)$ values become smaller, if they exist.

When analyzing the $B(E2)$ anomaly, both the ratio $B_{4/2}$ and absolute value of $B(E2;2_1^+\to 0_1^+)$ should be considered. If the nuclei ^{172}Pt, ^{168,170}Os , and ^{166}W with the $B(E2)$ anomaly are put in the isotopic evolutions [19–22], the results vary continuously. This is also key for considering these spectra as collective excitations. Extremely small $B(E2;2_1^+\to 0_1^+)$ values imply a large effective charge q, which may not be reasonable (see Ref. [52]).

D. Fourth example

In previous IBM versions, $O(5)$ symmetry exists when evolving from the $U(5)$ to $O(6)$ limits, which results in the crossover of the 0_2^+ and 0_3^+ states. When the parameters slightly deviate, significant energy level exclusion can occur [18]. This is important to confirm such phenomena. Recently, in the SU3-IBM, similar results were reported in Ref. [54]: it is a level-anticrossing phenomenon.

Important new results were reported recently. In Ref. [44], the $SU(3)$ quadrupole operator $\hat{Q}$ was replaced by the generalized quadrupole operator $\hat{Q}_\chi$. We also take ^{168}Os as an example, setting $\alpha = 0$, $\beta = -25.0$ keV, $\gamma = 0$, $\delta = 0$, $\eta = -26.9$ keV, $\zeta = 0$, $\xi = 43.65$ keV, and $\chi = -0.39$. For $SU(3)$ analysis, let $\chi = -\frac{\sqrt{7}}{2}$. Here, the

$SU(3)$ irrep. of the ground state is (16,0) with prolate shape. Fig. 4(a) shows the evolutional behaviors of the partial low-lying levels as functions of η from 0 to −53.8 keV; the middle point is the parameter reported in Ref. [44] ($\eta = -26.9$ keV). Intuitively, this evolutional behavior is similar to those in Fig. 1(a). The 4_1^+ state intersects with one other 4^+ state at $\eta = -44.8$ keV (red dashed lines), and the 6_1^+ state also intersects with one other 6^+ state at $\eta = -29.4$ keV (green dashed dotted lines). The two crossover points are marked by black circles. This means that this $B(E2)$ anomaly is also related with the $SU(3)$ symmetry.

Note that the middle point shows a normal $B_{4/2}$ value but is close to the anomalous region. This is interesting, revealing a new mechanism for the $B(E2)$ anomaly related with the level-anticrossing phenomenon. This new mechanism was discussed in detail in Ref. [66]. It was found that the $B(E2)$ anomaly in the $SU(3)$ symmetry limit and the $B(E2)$ anomaly along the transitional region from the $SU(3)$ symmetry limit to the $O(6)$ symmetry limit are closely related. These results can help further explain the anomalous small $B(E2;2_1^+ \to 0_1^+)$ value in ^{166}Os [60].

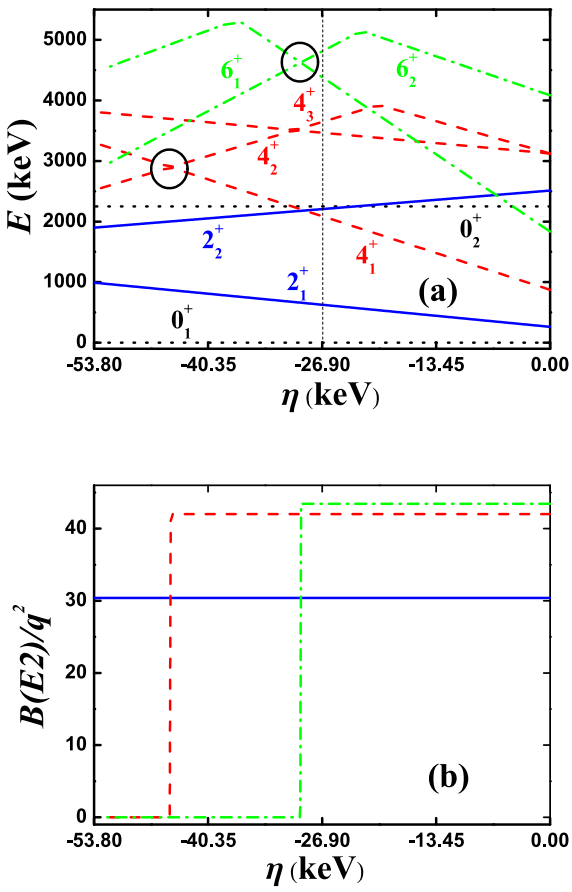

Fig. 4. (color online) (a) Evolutional behaviors of the partial low-lying levels as functions of η; (b) evolutional behaviors of $B(E2;2_1^+ \to 0_1^+)$ (blue real line), $B(E2;4_1^+ \to 2_1^+)$ (red dashed line), and $B(E2;6_1^+ \to 4_1^+)$ (green dashed dotted line) as functions of η. The parameters were deduced from Ref. [44].

A reasonable theory may be useful not only for explaining small $B_{4/2}$ values but also for considering normal $B(E2;2_1^+ \to 0_1^+)$ values in ^{172}Pt, ^{168,170}Os, and ^{166}W and for explaining the anomalous small $B(E2;2_1^+ \to 0_1^+)$ value in ^{166}Os [59]. This is addressed in Ref. [60].

E. Fifth example

In Ref. [46] , a new mechanism at the oblate side was reported. We also take ^{168}Os as an example, where $\alpha = 72.0$ keV, $\beta = -7.825$ keV, $\gamma = 2.636$ keV, $\delta = 0$, $\eta = 15.1$ keV, $\zeta = -1.09$ keV, and $\xi = 36.87$ keV. For $SU(3)$ analysis, let $\alpha = 0$. Here, the $SU(3)$ irrep. of the ground state is (0,8) with the oblate shape. Fig. 5(a) shows the evolutional behaviors of the partial low-lying levels as functions of η from 0 to 30.2 keV; the middle point is the parameter reported in Ref. [46] ($\eta = 15.1$ keV). Note that the 2_1^+ and 2_2^+ states intersect with each other at $\eta = 12.1$ keV (blue real lines), the 4_1^+ and 4_2^+ states intersect with each other at $\eta = 4.6$ keV (red dashed lines), and the 6_1^+ and 6_2^+ states intersect with each other at $\eta = 2.5$ keV (green dashed dotted lines). The three crossover points are marked by black circles. At the middle point, the $B_{4/2}$ value is infinity. This is interesting. We also confirm that this $B(E2)$ anomaly is related with the $SU(3)$ symmetry. This new mechanism is discussed in Section V in detail.

F. Brief summary

The results in the aforementioned five examples broaden our understanding of the $B(E2)$ anomaly. Even if the conditions that (1) the $B(E2;2_1^+ \to 0_1^+)$ value exists and (2) $B(E2;4_1^+ \to 2_1^+)$ is 0 are not satisfied in the $SU(3)$ symmetry limit, the $B(E2)$ anomaly may still appear.

If an explanation for the $B(E2)$ anomaly can include a $SU(3)$ symmetry limit, $SU(3)$ analysis should be performed. From the above examples and Refs. [40−47], we provide a great deal of new results. There are some phenomena that seem to have nothing to do with the $SU(3)$ symmetry but are actually related with it. This may be a more complicated mechanism that requires further elaboration (see Ref. [66]). In $SU(3)$ analysis, if no level-crossing occurs but the $B(E2)$ anomaly still appears, it can be attributed to the rigid triaxial rotor effect. The case in which no $B(E2)$ anomaly exists in the $SU(3)$ analysis but the $B(E2)$ anomaly appears when the d boson number operator is added (which is almost impossible), or $\hat{Q}$ is replaced by $\hat{Q}_\chi$, is critical. A general discussion will be provided with the extended Q-consistent Hamiltonian including up to fourth-order interactions. In a previous study [38], it was demonstrated that, for this extended Hamiltonian, when $\chi = 0$, that is, at the $O(6)$ symmetry limit, the $B(E2)$ anomaly cannot occur. Thus, it is import-

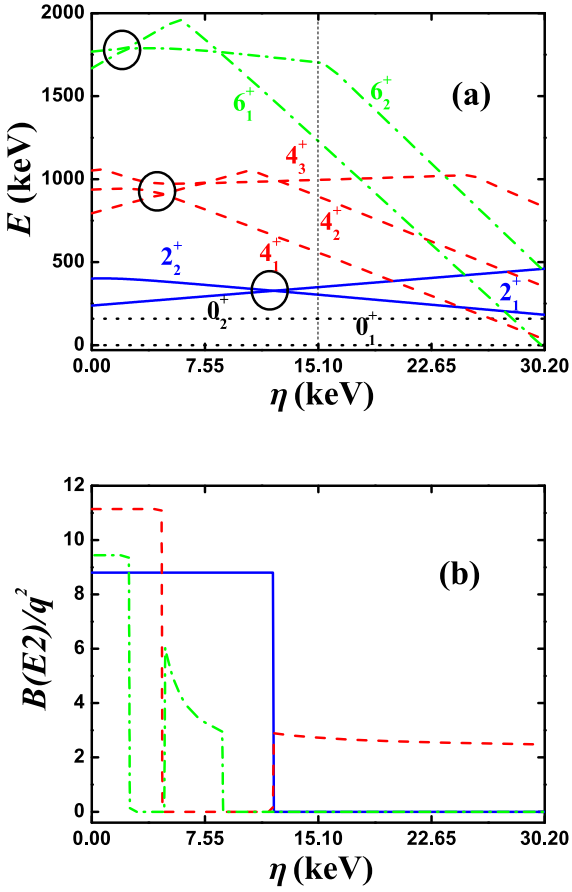

Fig. 5. (color online) (a) Evolutional behaviors of the partial low-lying levels as functions of η; (b) evolutional behaviors of $B(E2;2_1^+\to 0_1^+)$ (blue real line), $B(E2;4_1^+\to 2_1^+)$ (red dashed line), and $B(E2;6_1^+\to 4_1^+)$ (green dashed dotted line) as functions of η. The parameters were deduced from Ref. [46].

ant to discuss the evolving region from the *SU*(3) symmetry limit to the *O*(6) symmetry limit.

For the first and fourth examples, the values of the parameter η for the fourth-order interactions $[(\hat{L}\times\hat{Q})^{(1)}\times(\hat{L}\times\hat{Q})^{(1)}]^{(0)}$ are 0. Thus, the evolutional behaviors of the *B*(*E*2) values in Figs. 1(b) and 4(b) are simple. When these interactions are added, more complex evolutional behaviors can be observed, which is interesting. Although these interactions were studied within the context of the rigid triaxial explanation [41, 46, 47, 58], many details were inadequate. For the second and third examples, the sign of η is negative, and the evolutional behaviors of the *B*(*E*2) values in Figs. 2(b) and 3(b) become more complex (the evolution lines become curved). However, they are still similar to the cases in Figs. 1(b) and 4(b). For the fifth example, the sign of η is positive, and the evolutional behaviors of the *B*(*E*2) values in Fig. 5(b) become more complex than those in Figs. 2(b) and 3(b). Thus, further discussion on the $[(\hat{L}\times\hat{Q})^{(1)}\times(\hat{L}\times\hat{Q})^{(1)}]^{(0)}$ interaction is necessary to understand the more complex *B*(*E*2) anomaly, for example in ^{72,74}Zn [29−31] and ^{114}Te [32, 33].

V. FURTHER DISCUSSION

In this section, we further discuss the new mechanism presented in Fig. 5 [46]. In Fig. 5(b), the changes in the values of $B(E2;2_1^+\to 0_1^+)$ (blue real line), $B(E2;4_1^+\to 2_1^+)$ (red dashed line), and $B(E2;6_1^+\to 4_1^+)$ (green dashed dotted line) are similar to those in Fig. 1(b) but exhibit more complicated behaviors. The key for these behaviors is the introduction of the fourth-order interaction $[(\hat{L}\times\hat{Q})^{(1)}\times(\hat{L}\times\hat{Q})^{(1)}]^{(0)}$. The effect of the *SU*(3) fourth-order interactions on the *B*(*E*2) anomaly is complex, and a detailed discussion will be addressed in the future. Here, just the parameters reported in Ref. [46] are considered. We can see that the fourth-order interaction brings in new features.

In Fig. 5(b), when $\eta = 15.1$ keV (the parameter used was reported in Ref.[46]), $B(E2;2_1^+\to 0_1^+)=0$ while

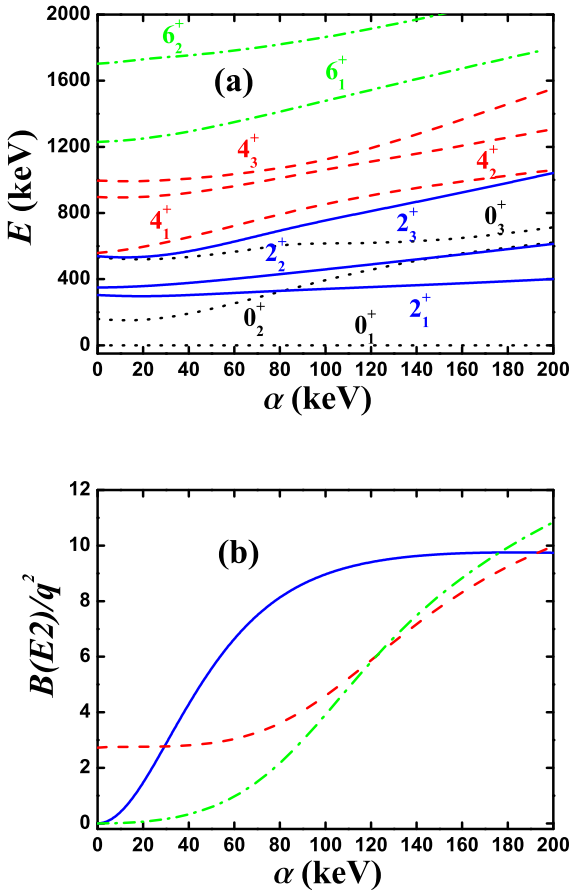

Fig. 6. (color online) (a) Evolutional behaviors of the partial low-lying levels as functions of α; (b) evolutional behaviors of $B(E2;2_1^+\to 0_1^+)$ (blue real line), $B(E2;4_1^+\to 2_1^+)$ (red dashed line), and $B(E2;6_1^+\to 4_1^+)$ (green dashed dotted line) as functions of α. The parameters were deduced from Ref. [46] ($\eta = 15.1$ keV).

$B(E2;4_1^+ \to 2_1^+) \neq 0$. Thus, $B_{4/2} = \infty$, which is a new result. When $\eta = 11.325$ keV, $B(E2;2_1^+ \to 0_1^+) \neq 0$ while $B(E2;4_1^+ \to 2_1^+) = 0$. Thus, $B_{4/2} = 0$, which was reported in a previous study. For both cases, $B(E2;6_1^+ \to 4_1^+) = 0$. When $\eta = 7.55$ keV, $B(E2;2_1^+ \to 0_1^+) \neq 0$, $B(E2;4_1^+ \to 2_1^+) = 0$ while $B(E2;6_1^+ \to 4_1^+) \neq 0$. When the fourth-order interaction is introduced, any $B(E2)$ results may be obtained.

The evolutional trends are similar. Figs. 6–8(b) show the evolutional behaviors of the values of $B(E2;2_1^+ \to 0_1^+)$, $B(E2;4_1^+ \to 2_1^+)$, and $B(E2;6_1^+ \to 4_1^+)$ as functions of α when $\eta = 15.1$, 11.325, and 7.55 keV. The evolutional trends are notably different.

Fig. 9 presents the evolutional behaviors of the $B_{4/2}$ values as functions of α for $\eta = 15.1$ keV, $\eta = 11.325$ keV, and $\eta = 7.55$ keV. Other parameters were deduced from Ref. [46]. In ^{168}Os, $B_{4/2} = 0.34$. For $\eta = 15.1$ keV, the smallest value is 0.45. In Ref. [46], $B_{4/2} = 0.53$ was used. In the following section, $B_{4/2} = 0.45$ is used for result 1 (black point). For $\eta = 11.325$ keV and 7.55 keV, $B_{4/2} = 0.34$ exists (blue and red points) and is used for results 2 and 3. For comparison, $B_{4/2} = 0$ is also used for result 4 when $\eta = 7.55$ keV, which is just the result of $SU(3)$ analysis on result 3.

VI. $B(E2)$ ANOMALY IN ^{168}OS

If the fourth-order interaction $[(\hat{L}\times\hat{Q})^{(1)}\times(\hat{L}\times\hat{Q})^{(1)}]^{(0)}$ is not added, the $B(E2)$ values of each energy level in the yrast band can gradually decrease as the angular momentum L increases [40, 58]. However, when this interaction is added, this change becomes more irregular. This is important for understanding irregular $B(E2)$ anomalies.

Results 1 – 3 correspond to the three points (black, blue, and red) in Fig. 9. Result 4 corresponds to the $\alpha = 0$ point of the red line in Fig. 9. Let the energy of the 2_1^+ state be equal to the experimental one in ^{168}Os. The parameters of the four results are shown in Table 1 and the fitting values are listed in Table 2. For results 1, 2, and 3,

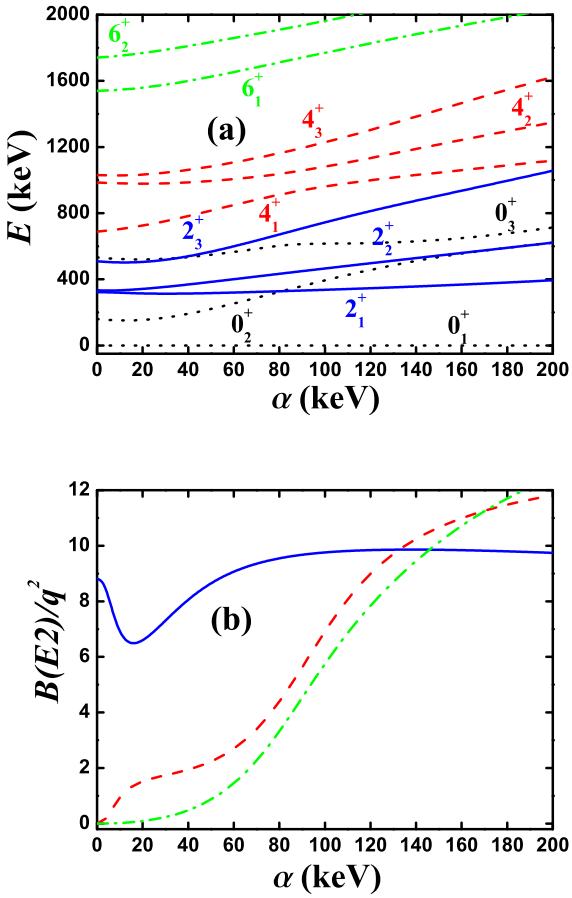

Fig. 7. (color online) (a) Evolutional behaviors of the partial low-lying levels as functions of α; (b) Evolutional behaviors of $B(E2;2_1^+ \to 0_1^+)$ (blue real line), $B(E2;4_1^+ \to 2_1^+)$ (red dashed line), and $B(E2;6_1^+ \to 4_1^+)$ (green dashed dotted line) as functions of α. The parameters were deduced from Ref. [46] but $\eta = 11.325$ keV.

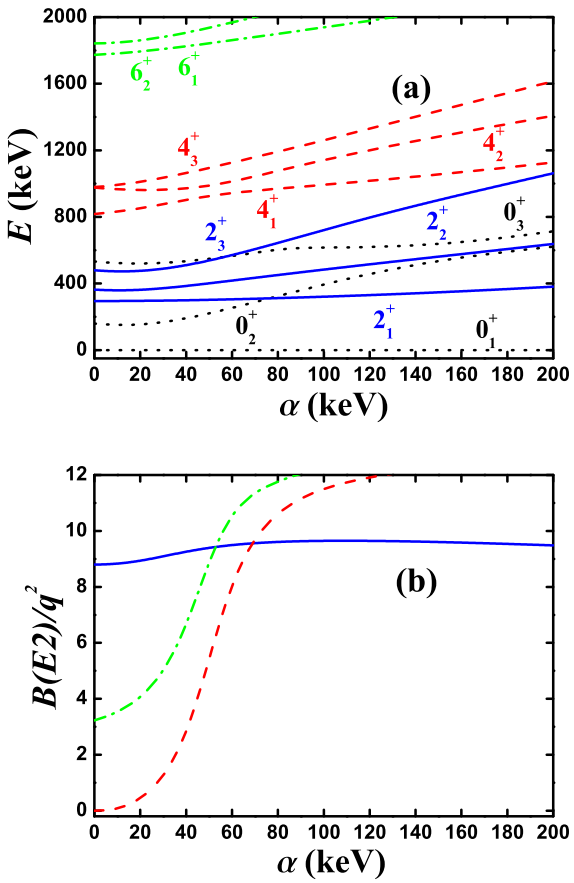

Fig. 8. (a) Evolutional behaviors of the partial low-lying levels as functions of α; (b) evolutional behaviors of $B(E2;2_1^+ \to 0_1^+)$ (blue real line), $B(E2;4_1^+ \to 2_1^+)$ (red dashed line), and $B(E2;6_1^+ \to 4_1^+)$ (green dashed dotted line) as functions of α. The parameters were deduced from Ref. [46] but $\eta = 7.55$ keV.

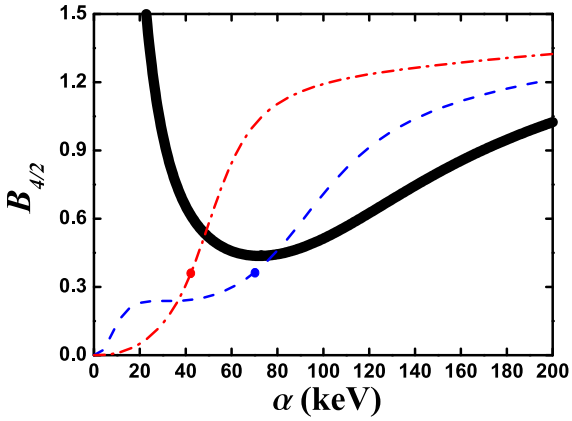

Fig. 9. Evolutional behaviors of the $B_{4/2}$ values as functions of α for $\eta = 15.1$ keV (black real line), $\eta = 11.325$ keV (blue dashed dotted line), and $\eta = 7.55$ keV (red dashed dotted line). Other parameters were deduced from Ref. [46].

the energies of the 0_2^+ and 2_2^+ states increase. For results 1 and 2, the values of $B(E2;8_1^+ \to 6_1^+)$ are larger. For result 3, the value of $B(E2;6_1^+ \to 4_1^+)$ is larger. Thus, these $B(E2)$ values are sensitive to the parameters. For result 4, the results of the *SU*(3) analysis are shown. The irregularity of the $B(E2)$ values is clear when L increases. When $\hat{n}_d$ is added, result 4 becomes result 3, which exhibits a better fitting effect. Level-crossing is indeed a possible reason for the emergence of the $B(E2)$ anomaly. For a better understanding of the $B(E2)$ anomaly in ^{168}Os, more experimental results are needed.

VII. CONCLUSION

In this study, we proposed a powerful technique for understanding the $B(E2)$ anomaly, namely the *SU*(3) analysis. By analyzing the examples in Refs. [40–47], new results were obtained. Three of these results are particularly relevant. First, the *SU*(3) third-order interaction $[L\times Q\times L]^{(0)}$ is critical for the *SU*(3) anomaly. Whether this relationship is unique requires further investigation. Second, when this interaction is added, various level-crossing phenomena can occur. The causes of the $B(E2)$ anomaly in realistic experiments require more experimental research. Searching for additional mechanisms for the $B(E2)$ anomaly also seems necessary. Third, not only the value of $B(E2;4_1^+ \to 2_1^+)$ but also those of $B(E2;6_1^+ \to 4_1^+)$ and $B(E2;2_1^+ \to 0_1^+)$ can be anomalous. The $B(E2)$ anomaly in ^{168}Os was discussed. It is critical to obtain more experimental $B(E2)$ anomaly results.

Table 1. Parameters of the four results for fitting ^{168}Os. The unit is keV.

	α	β	γ	η	ζ	ξ
Res. 1	63.72	-6.23	2.33	13.37	-0.97	41.66
Res. 2	91.58	-10.73	3.62	15.53	-1.50	33.69
Res. 3	107.48	-20.41	6.88	19.70	-2.85	15.36
Res. 4	0	-13.52	4.55	13.05	-1.89	35.93

Table 2. Experimental and fitting values of the four results for ^{168}Os. The unit of the energy level is keV whereas that of the $B(E2)$ value is W.u.. The effective charges of results 1-4 are 3.114 $\sqrt{\text{W.u.}}$, 2.2825 $\sqrt{\text{W.u.}}$, 2.823 $\sqrt{\text{W.u.}}$, and 2.900 $\sqrt{\text{W.u.}}$, respectively.

	Exp.	Res. 1	Res. 2	Res. 3	Res. 4
$E_{2_1^+}$	341	341	341	341	341
$E_{4_1^+}$	857	857	857	867	857
$E_{6_1^+}$	1499	1607	1586	1642	1898
$E_{8_1^+}$	2223	2342	2136	2103	2771
$E_{10_1^+}$	2983	3522	3248	2960	4213
$E_{0_2^+}$		261	380	521	276
$E_{2_2^+}$		424	463	575	461
$E_{3_1^+}$		778	821	962	841
$E_{4_2^+}$		1057	1055	1064	1130
$B(E2;2_1^+ \to 0_1^+)$	74(13)	74	74	74	74
$B(E2;4_1^+ \to 2_1^+)$	25(13)	33	25	25	0
$B(E2;6_1^+ \to 4_1^+)$		16	16	50	27
$B(E2;8_1^+ \to 6_1^+)$		57	49	11	0
$B(E2;10_1^+ \to 8_1^+)$		2.8	2.8	22	14

References

[1] A. Arima and F. Iachello, Phys. Rev. Lett. **35**, 1069 (1975)
[2] F. Iachello and A. Arima, *The Interacting Boson Model* (Cambridge: Cambridge University Press, 1987)
[3] J. Jolie, R. F. Casten, P. von Brentano *et al.*, Phys. Rev. Lett. **87**, 162501 (2001)
[4] D. Warner, Nature **420**, 614 (2002)
[5] R. F. Casten, Nat. Phys. **2**, 811 (2006)
[6] R. F. Casten and E. A. McCutchan, J. Phys. G: Nucl. Part. Phys. **34**, R285 (2007)
[7] D. Bonatsos and E. A. McCutchan, Nucl. Phys. News **19**, 13 (2009)
[8] R. F. Casten, Prog. Part. Nucl. Phys. **62**, 183 (2009)
[9] P. Cejnar and J. Jolie, Prog. Part. Nucl. Phys. **62**, 210 (2009)
[10] P. Cejnar, J. Jolie and R. F. Casten, Rev. Mod. Phys. **82**, 2155 (2010)
[11] R. V. Jolos and E. A. Kolganova, Phys.-Usp. **64**, 325 (2021)
[12] L. Fortunato, Prog. Part. Nucl. Phys. **121**, 103891 (2021)
[13] P. Cejnar, P. Stránský, M. Macek *et al.*, J. Phys. A: Math. Theor. **54**, 133001 (2021)
[14] D. Bonatsos, A. Martinou, S. K. Peroulis *et al.*, Phys. Scr. **99**, 062003 (2024)

[15] P. Cejnar and J. Jolie, Phys. Rev. C **61**, 6237 (2000)
[16] P. Cejnar, S. Heinze, and J. Jolie, Phys. Rev. C **68**, 034326 (2003)
[17] F. Iachello and N. V. Zamfir, Phys. Rev. Lett. **92**, 212501 (2004)
[18] F. Pan, T. Wang, Y. S. Huo *et al.*, J. Phys. G: Nucl. Part. Phys. **35**, 125105 (2008)
[19] T. Grahn, S. Stolze, D. T. Joss *et al.*, Phys. Rev. C **94**, 044327 (2016)
[20] B. Sayğı, D. T. Joss, R. D. Page *et al.*, Phys. Rev. C **96**, 021301(R) (2017)
[21] B. Cederwall, M. Doncel, Ö. Aktas *et al.*, Phys. Rev. Lett. **121**, 022502 (2018)
[22] A. Goasduff, J. Ljungvall, T. R. Rodrguez *et al.*, Phys. Rev. C **100**, 034302 (2019)
[23] P. E. Garrett, K. L. Green and J. L. Wood, Phys. Rev. C **78**, 044307 (2008)
[24] P. E. Garrett, J. Bangay, A. Diaz Varela *et al.*, Phys. Rev. C **86**, 044304 (2012)
[25] J. C. Batchelder, N. T. Brewer, R. E. Goans*et al.*, Phys. Rev. C. **86**, 064311 (2012)
[26] P. E. Garrett, T. R. Rodríguez, A. Diaz Varela*et al.*, Phys. Rev. Lett. **123**, 142502 (2019)
[27] P. E. Garrett, T. R. Rodríguez, A. Diaz Varela*et al.*, Phys. Rev. C **101**, 044302 (2020)
[28] P. E. Garrett, J. L. Wood and S. W. Yates, Phys. Scr. **93**, 063001 (2018)
[29] C. Louchart, A. Obertelli, A. Görgen *et al.*, Phys. Rev. C **87**, 054302 (2013)
[30] A. Illana, M. Zielińska, M. Huyse *et al.*, Phys. Rev. C **108**, 044305 (2023)
[31] S. Hellgartner, D. Mücher, K. Wimmer*et al.*, Phys. Lett. B **841**, 137933 (2023)
[32] O. Möller, N. Warr, J. Jolie*et al.*, Phys. Rev. C **71**, 064324 (2005)
[33] Prithwijita Ray, H. Pai, Sajad Ali *et al.*, Phys. Rev. C **101**, 064313 (2020)
[34] T. Otsuka, Y. Tsunoda, T. Abe*et al.*, Phys. Rev. Lett. **123**, 222502 (2019)
[35] Y. Tsunoda and T. Otsuka, Phys. Rev. C **103**, L021303 (2021)
[36] T. Otsuka, Y. Tsunoda, Y. Utsuno*et al.*, Eur. Phys. J. A **61**, 126 (2025)
[37] J. Jolie and A. Linnemann, Phys. Rev. C **68**, 031301(R) (2003)
[38] T. Wang, Chin. Phys. C **46**, 074101 (2022)
[39] T. Wang, X. Chen and Y. Zhang, Chin. Phys. C **49**, 014107 (2025)
[40] T. Wang, EPL **129**, 52001 (2020)
[41] Y. Zhang, Y. W. He, D. Karlsson*et al.*, Phys. Lett. B **834**, 137443 (2022)
[42] T. Wang, Phys. Rev. C **107**, 064303 (2023)
[43] Y. Zhang, S. N. Wang, F. Pan*et al.*, Phys. Rev. C **110**, 024303 (2024)
[44] F. Pan, Y. Zhang, Y. X. Wu*et al.*, Phys. Rev. C **110**, 054324 (2024)
[45] W. Teng, Y. Zhang and C. Qi, Chin. Phys. C **49**, 014102 (2025)
[46] Y. Zhang and W. Teng, Phys. Rev. C **111**, 014324 (2025)
[47] W. Teng, Y. Zhang, S. N. Wang*et al.*, Phys. Lett. B **865**, 139487 (2025)
[48] W. Teng, S. N. Wang, Y. Zhang *et al.*, accepted by Chin. Phys. C
[49] T. Wang, arXiv: 2501.10925v2
[50] L. Fortunato, C. E. Alonso, J. M. Arias *et al.*, Phys. Rev. C **84**, 014326 (2011)
[51] Y. Zhang, F. Pan, Y. X. Liu*et al.*, Phys. Rev. C **85**, 064312 (2012)
[52] T. Wang, B. C. He, D. K. Li *et al.*, Phys. Rev. C **78**, 064322 (2023)
[53] T. Wang, B. C. He, C. X. Zhou*et al.*, Chin. Phys. C **48**, 094102 (2024)
[54] C. X. Zhou and T. Wang, Phys. Rev. C **108**, 024309 (2023)
[55] T. Wang, C. X. Zhou and L. Fortunato, arXiv: 2412.14881v1
[56] C. X. Zhou and T. Wang, in preparation
[57] D. H. Zhao, X. S. Kang, L. Gong *et al.*, arXiv: 2504.06571
[58] Y. Zhang, F. Pan, L. R. Dai*et al.*, Phys. Rev. C **90**, 044310 (2014)
[59] S. Stolze, T. Grahn, R. Julin *et al.*, J. Phys. G: Nucl. Part. Phys. **48**, 125101 (2021)
[60] C. G. Zhang, S. C. Jin, T. Wang *et al.*, submitted
[61] Y. Leschber and J. P. Draayer, Phys. Lett. B **190**, 1 (1987)
[62] O. Castaños, J. P. Draayer and Y. Leschber, Com. Phys. Comm. **52**, 71 (1988)
[63] O. Castaños, J. P. Draayer and Y. Leschber, Z. Phys. A **329**, 33 (1988)
[64] G. Vanden Berghe, H. E. De Meyer and P. Van Isacker, Phys. Rev. C **32**, 1049 (1985)
[65] Y. F. Smirnov, N. A. Smirnova and P. Van Isacker, Phys. Rev. C **61**, 041302(R) (2000)
[66] T. Wang, Y. X. Cheng, D. K. Li *et al.*, arXiv: 2503.22100